# Systematics of two-component superconductivity in $YBa_2Cu_3O_{6.95}$ from microwave measurements of high-quality single crystals

H. Srikanth, Z. Zhai, and S. Sridhar
*Department of Physics, Northeastern University, 360 Huntington Avenue, Boston, Massachusetts 02115*

A. Erb and E. Walker
*DPMC, Université de Genève, Genève, Switzerland*

(Received 8 September 1997)

A systematic set of measurements of the microwave (10 GHz) surface impedance ($Z_s=R_s+iX_s$) of twinned $YBa_2Cu_3O_{6.95}$ single crystals (called YBCO/BZO) grown in $BaZrO_3$ crucibles reveal properties that are not directly seen in similar measurements on other YBCO samples. The complex conductivity $\sigma=\sigma_1-i\sigma_2$ obtained as a function of temperature ($T$) from the surface impedance data shows two key features : (1) A conductivity peak in $\sigma_1(T)$ around 80 K in addition to peaks at 30 K and 92 K and (2) extra pairing below 65 K in addition to the onset of pairing below the bulk $T_c$ of 93.4 K as revealed in $\sigma_2(T)$. These features are present in all three YBCO/BZO crystals measured and are absent in YBCO crystals grown by other methods. These results show that in addition to pairing at $T_c=$ 93.4 K, an additional pairing channel opens up at ($\sim$65 K). High-pressure oxygenation of one of the crystals still yields the same results, and shows that the data cannot be due to unwanted macroscopic segregation of O-deficient regions. Systematics on three single crystals show that the height of the quasiparticle conductivity peak at 80 K in the superconducting state is correlated with the inelastic scattering rate in the normal state. Close to $T_c$, $\sigma_2(T)\sim(T_c-T)$, indicating a mean-field behavior and inconsistent with $3DXY$ fluctuations over a wide temperature range. A single complex order parameter cannot describe these data, and the results suggest that at least two superconducting components with corresponding pairing temperature scales ($T_A\sim$65 K and $T_B=T_c=$93.4 K) are required. Comparison to model calculations considering various decoupled two-component scenarios ($A+B=d+s,s+d,d+d$) are presented. The comparison shows that the experimental data do not distinguish between these various scenarios, however, the data do require that one of the components be an order parameter with nodes in the gap, such as a $d$-wave order parameter. Fit parameters to the calculations using the different scenarios are presented. These components are naturally present in all YBCO samples, however, impurities appear to suppress the pair density of the low-temperature $A$ component and lead to greatly enhanced scattering of the high-temperature $B$ component. Overall, our results strongly suggest the presence of multiple pairing temperature scales and energies in $YBa_2Cu_3O_{6.95}$. [S0163-1829(98)00513-X]

## I. INTRODUCTION

The order parameter of high-temperature superconductors has been extensively studied recently, and a consensus seems to have emerged in favor of a $d$-wave order parameter.[1] However, there are some notable indications (see Refs. 2,3 for a summary) which suggest that, particularly in the most widely studied material $YBa_2Cu_3O_{6.95}$, a pure $d$-wave order parameter may not occur and that there are indications of a multi-component order parameter (e.g., $s+d$).

Material purity is crucial for studies of fundamental physical properties not obscured by impurity-related artifacts. This fact has been validated time and again in experiments on oxide superconductors as well as other materials. It is now accepted that improvement in material quality has often resulted in a better understanding of the physical properties in solid state systems.

The recent growth of $YBa_2Cu_3O_{7-\delta}$ single crystals in $BaZrO_3$(BZO) crucibles has ushered in a new generation of ultrapure samples.[4] This growth method avoids the critical problem of crucible corrosion and leads to single crystals with extremely clean surfaces and purity exceeding 99.995%. In contrast, the best crystals grown in conventional crucibles such as Au and yttria-stabilized-zirconia (YSZ) have final reported purities of 99.5$-$99.95 %.[5,6] A number of experiments on YBCO/BZO crystals have revealed features which are either greatly suppressed or not present in YBCO/YSZ samples. We have recently observed features in the microwave surface impedance of YBCO/BZO which clearly indicates the presence of two superconducting components.[7]

In this paper, we present further evidence on the systematics in three YBCO/BZO crystals. The results obtained confirm our earlier findings,[7] viz., (1) a conductivity peak in $\sigma_1(T)$ around 80 K which is correlated with the normal state scattering rate and (2) extra pairing below 65 K in addition to onset of pairing below the bulk $T_c$ of 93.4 K as revealed in $\sigma_2(T)$. A single complex order parameter cannot describe these data and the data indicate the presence of at least two pairing processes, leading to at least two order parameter components. Model calculations considering various simple two-component scenarios (decoupled $d+s$ and $d+d$) are presented. We show that the two-component picture can provide a quantitative description of the data, whereas a single

 

TABLE I. A comparison of some material and physical properties of YBCO/BZO and YBCO/YSZ single crystals.

| YBCO/YSZ | YBCO/BZO |
|---|---|
| Crucible: yttria-stabilized zirconia (YSZ) | Crucible: $BaZrO_3$ |
| Crystal purity: 99.5 to 99.95% (Ref. 5) | Crystal purity: 99.995% (Ref. 8) |
| $T_c = 93.2$ to 93.5 K | $T_c = 93.2$ to 93.5 K |
| Estimated $\lambda(0) \sim 1600-2000$ Å | Estimated $\lambda(0) \sim 1000-1400$ Å |
| Flux lattice not imaged with STM | Flux lattice imaged with cryogenic STM (Ref. 11) |
| Schottky anomaly present in specific heat | Schottky anomaly eliminated in high pressure oxygenated $O_7$ (Ref. 15) |
| Large ''fishtail effect'' in magnetization | ''Fishtail'' greatly suppressed in high pressure oxygenated $O_{6.95}$ and eliminated in $O_7$ (Ref. 12) |
| Substantial pinning due to impurities | Very low pinning evidenced by extremely low critical currents (Ref. 16) and observation of flux lattice melting (Ref. 15) |

order parameter (of any symmetry) does not. In addition the two-component picture can provide a description of the data on the earlier generation of YBCO/YSZ crystals also. Analysis of the data close to $T_c$ is not consistent with $3DXY$ fluctuations and displays a mean-field behavior. Systematics on three twinned single crystals show a correlation between the inelastic scattering rate in the normal state with the quasiparticle conductivity peak at 80 K in the superconducting state. We show that while a $T$-dependent scattering rate is required to quantitatively describe the conductivity peaks, the two-component scenario provides a natural explanation for the location of the 30 and 80 K peaks in $\sigma_1(T)$ as arising from pairing at 65 K and 93 K, respectively, in contrast with earlier interpretation of YBCO/YSZ data which associated the 30 K peak with pairing at 93 K. Overall, our results show that a pure $d$-wave state does not occur in $YBa_2Cu_3O_{6.95}$ and strongly suggest the presence of multiple pairing energies. We note that several microscopic pairing scenarios are consistent with the conclusions of this paper.

*Properties of* YBCO/BZO *crystals.* One of the causes for the presence of impurities in $YBa_2Cu_3O_{7-\delta}$ single crystals is the random substitution at the Cu chain sites by trace amounts of crucible constituents such as Au during the melt growth process. This results in local variation of oxygen vacancy distribution, introduction of magnetic moments and other local defects.[8–10] Although the overall $T_c$ and sharpness of the superconducting transition may not be affected by a combination of these elements associated with impurities, important features of the superconducting ground state such as the order parameter symmetry, scattering, superfluid density, etc., are likely to be influenced. It is precisely these local impurities which are eliminated in (BZO) grown $YBa_2Cu_3O_{7-\delta}$ (YBCO) crystals thus providing an opportunity to probe the intrinsic ground state properties free from defects. Elimination of the metallic impurities also leaves oxygen stoichiometry as the only variable which needs to be controlled.[8]

It is important to emphasize at this juncture that several new results have been obtained on these new generation crystals by a number of experimenters using a variety of probes such as thermal, magnetic, and electrodynamic response, and have led to a clearer picture of the nature of superconductivity in $YBa_2Cu_3O_{6.95}$. Some of these results are as follows.

(1) Direct imaging of the flux lattice of YBCO using low-temperature scanning tunnel microscopy (STM).[11] Thus far this has only been feasible with the YBCO/BZO crystals.

(2) ''Fishtail effect'' in magnetization *eliminated* in high-pressure oxygen annealed $YBCO_{7.0}$/BZO and optimally doped YBCO/BZO samples.[12]

(3) Schottky contribution to specific heat *suppressed* in $YBCO_{7.0}$/BZO indicating the total absence of magnetic moments.[13]

(4) The microwave conductivities $\sigma_1(T)$ and $\sigma_2(T)$ exhibit *two* distinct features not consistent with a single superconducting order parameter.[7]

(5) The vortex lattice imaged with STM shows two different regions which is either representative of two superconducting components or two types of ordered oxygen clusters.[14]

(6) Clear observation of a direct first order melting transition in $YBCO_{7.0}$/BZO from a vortex lattice to liquid without an intervening glassy state.[15]

(7) Evidence of extremely low $J_c$ in $YBCO_{7.0}$/BZO crystals indicative of very low pinning.[16]

In an attempt to bring forth the essential differences, we have presented a comparison of some material and physical properties of YBCO/YSZ and YBCO/BZO crystals in Table I.

## II. EXPERIMENTAL RESULTS

The microwave measurements were carried out in a 10 GHz Nb cavity using a ''hot finger'' technique.[17] We measure the surface impedance $Z_s = R_s + iX_s$ and penetration depth $\lambda (= X_s/\mu_0\omega)$ as functions of temperature $T$, from which we extract the complex conductivity $\sigma_s = \sigma_1 - i\sigma_2$. This method has been extensively validated by a variety of measurements on cuprates and borocarbide superconductors.[18,19]

Three single crystals (labeled AE103, AE105, and AE180 and typically $1.3 \times 1.3 \times 0.1 \text{mm}^3$ in size) from different batches grown in BZO crucibles and one crystal (labeled AEXX) of comparable dimensions grown in a YSZ crucible

were measured to study the systematics in the different samples. While standard oxygen annealing procedures at atmospheric pressure were followed to obtain optimally doped crystals with oxygen stoichiometry around $O_{6.95}$ in AE103, AE105, and AEXX, the AE180 sample was annealed at a pressure of 100 bars for 20 h at 700 °C. Note that this high-pressure annealing results in elimination of the formation of oxygen vacancy clusters and as a consequence, the ''fish-tail'' anomaly in magnetization is suppressed. The crystals (AE103, AE105, and AE180) grown in BZO had $T_c = 93.4$ K and AEXX had $T_c = 92.4$ K. All four crystals exhibited very narrow transitions in $R_s(T)$ at 10 GHz of $< 0.3$ K. The crystals are typically twinned and a study of detwinned samples is the subject of future work.

The temperature dependence of the surface resistance $R_s(T)$ and change in penetration depth $\Delta\lambda(T)$ were presented for AE103 and AEXX crystals and discussed in detail in an earlier publication.[7] In this paper, we show that the data for AE105 and AE180 crystals also show the features seen in the AE103 single crystal. The data for all the three high-purity YBCO/BZO crystals clearly reveal a bump in the vicinity of 60 K which is not seen in YBCO/YSZ. Also the estimated London penetration depth $\lambda(0)$ for YBCO/BZO samples are $\simeq 1000$ Å which is lower than the value of 1400 Å estimated for the YBCO/YSZ crystal. We obtain the absolute value of $X_s$ by equating $R_n = X_n$ above $T_c$.

Since the absolute values of $R_s(T)$ and $X_s(T)$ are now known, we can plot the amplitude $|Z_s(T)| \equiv \sqrt{R_s(T)^2 + X_s(T)^2}$as a function of $T$. Figure 1 shows such a plot for the three YBCO/BZO samples along with YBCO/YSZ for comparison. The virtue of plotting $|Z_s(T)|$ is that one can clearly see the lower $\lambda(0)$ in YBCO/BZO which effectively translates to a higher superfluid density $(n_s/m) \sim 1/\lambda^2$.

In the superconducting state, the complex surface impedance is related to the complex conductivity and penetration depth: $Z_s = R_s + iX_s = \sqrt{i\mu_0\omega/(\sigma_1 - i\sigma_2)}$. Since the absolute values of $R_s$ and $X_s$ are known, it is possible to extract the complex conductivities:

$$\sigma_1 = \frac{2\mu_0\omega R_s X_s}{(2R_sX_s)^2 + (R_s^2 - X_s^2)^2},$$

$$\sigma_2 = \frac{\mu_0\omega(X_s^2 - R_s^2)}{(2R_sX_s)^2 + (R_s^2 - X_s^2)^2}.$$

These quantities are important because they enable comparison with microscopic theories. The pair conductivity $\sigma_2$ is a representation of the superfluid density $\sigma_2 = [\mu_0\omega\lambda^2(T)]^{-1}$ and is a convenient way of probing how the condensate builds up below the superconducting transition. The quasiparticle conductivity $\sigma_1$ is determined by the quasiparticle density as well as the quasiparticle scattering time.

In Fig. 2, the temperature dependence of $\sigma_1(T)$ and $\sigma_2(T)$ are plotted for all the four samples AE103, AE105, AE180, and AEXX. The two following features emerge clearly from a comparison of the data.

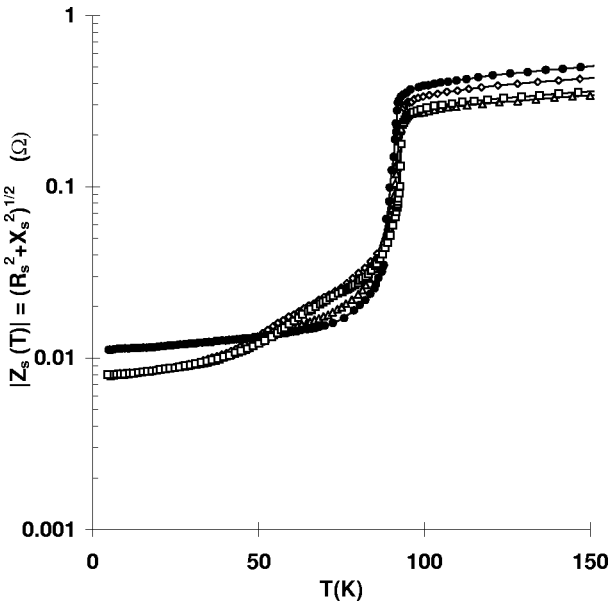


FIG. 1. Magnitude of surface impedance amplitude $|Z_s(T)|$ of YBCO/BZO and YBCO/YSZ single crystals. Open symbols are used for BZO grown crystals: AE103 (open squares), AE180 (open triangles), and AE105 (open diamonds). The data for YSZ grown AEXX (filled circles) is also shown. The plot emphasizes the fact that $\lambda(0)$ for all the YBCO/BZO crystals is lower than that of YBCO/YSZ.

(i) $\sigma_2(T)$ shows two distinct regions of variation above and below $\sim 60-70$ K in AE103, AE105, and AE180 samples in comparison with AEXX. Given the fact that $\lambda(0)$ is lower in YBCO/BZO this implies enhanced pair conductivity in these samples.

(ii) The normal conductivity $\sigma_1(T)$ shows a peak at around 80 K$(\sim 0.9T_c)$ in YBCO/BZO crystals which is absent in YBCO/YSZ. This peak is greatly suppressed in AE105 as seen in Fig. 2. We show later that there is a correlation between this peak and the normal state inelastic scattering rate of the samples. It is to be noted that the normal conductivity peak at $\sim 30-35$ K and a very sharp peak near $T_c$ (see inset in bottom panel of Fig. 2) are present in all the samples .

Note that these two features are both absent in all previously measured crystals. This is evident from the data on the YBCO/YSZ sample shown in Fig. 2. We emphasize that the YBCO/YSZ data is indeed ''canonical'' of the samples prepared by previous growth methods. This is illustrated in Fig. 3 which compares the YBCO/YSZ data with that measured by us on a detwinned $LuBa_2Cu_3O_{6.95}$ sample[20] and by the UBC group on $YBa_2Cu_3O_{6.95}$.[21] Note the excellent consistency of data on all previous samples with each other in Fig. 3, and the systematic differences with the new data in Fig. 2.

## III. ANALYSIS AND DISCUSSION

A calculation of the high-frequency conductivity requires proper incorporation of scattering effects along with self-consistent calculations of the gap and density of states. In addition anisotropy effects should also be included for the cuprate superconductors. While this has been done[22–24] for

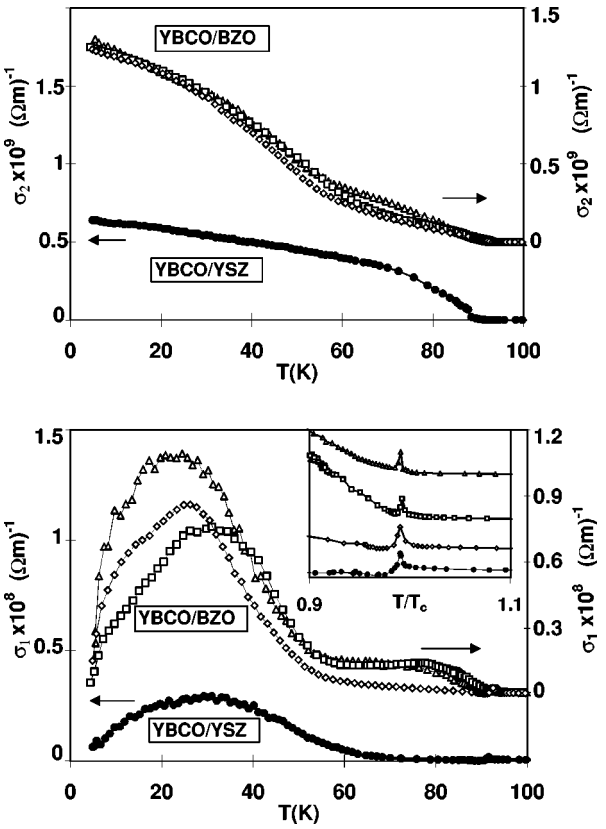


FIG. 2. Complex conductivities $\sigma_2$ (top panel) and $\sigma_1$ (bottom panel). The YBCO/BZO data are shown in open symbols and the YBCO/YSZ data in filled circles. Note the extra pairing at around 60 K in $\sigma_2$ and the peak at 80 K in $\sigma_1$ in YBCO/BZO, both absent in YBCO/YSZ data. Inset of bottom panel shows an exploded view of the region near $T_c$ to highlight the presence of the sharp peak in all samples.

unconventional superconductors including those with a $d$-wave order parameter, these approaches are not easily amenable to comparison with experimental data.

Instead, in order to compare with the present experimental data we use a simpler ''two-fluid'' model of the form:[25]

$$\sigma(\omega,T)=\sigma_1-i\sigma_2=\frac{ne^2}{m}\left[\frac{f_n}{1/\tau(T)}-\frac{if_s}{\omega}\right],$$

where $f_n$ and $f_s$ represent the fractions of normal and superfluid (with $f_n+f_s=1$), and $\tau$ is the relaxation time for normal electrons. In this model, the normal electrons have damping with the usual Drude conductivity at high frequencies, and the superconducting electrons have inertia but no damping. The quasiparticle and pair conductivities can be numerically calculated from

$$f_s=(1-f_n)=1-2\left\langle\int_0^\infty\left(-\frac{\partial f}{\partial E}\right)d\epsilon\right\rangle,$$

where $E=\sqrt{\epsilon^2+\Delta^2(\phi,T)}$, and $\Delta(\phi,T)$ is the gap parameter, and $\langle\cdots\rangle=\int_0^{2\pi}d\phi$ indicates an angular average over $\phi$. The gap parameters are given by $\Delta(\phi,T)=\Delta_s(T)$ and $\Delta(\phi,T)=\Delta_d(T)\cos(2\phi)$ for $s$-wave and $d$-wave superconductors, respectively. For $\Delta_s(T)$ and $\Delta_d(T)$ we use appropriate mean-field temperature dependences. The validity of this two-fluid approach, which is used frequently in $s$-wave superconductors following Mattis and Bardeen,[26] has been discussed for $d$-wave superconductors by Hirschfeld *et al.*[23]

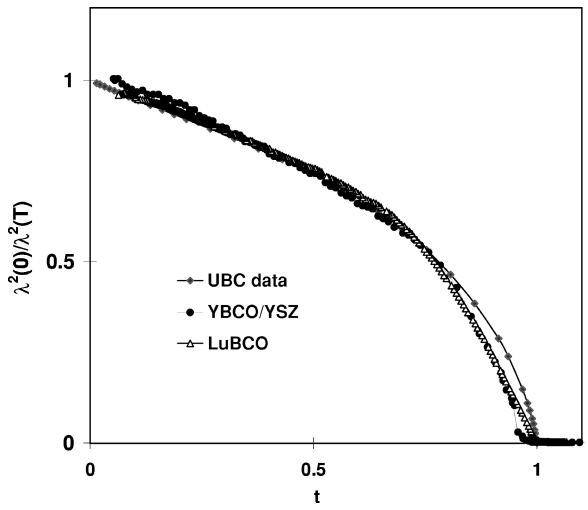


FIG. 3. Superfluid density of the YBCO/YSZ single crystal (AEXX) plotted against reduced temperature. Data for an untwinned YSZ grown LuBCO crystal and the UBC data are also shown for comparison.

### A. Comparison with models

We now discuss the comparison of the experimental data with detailed models which are implemented assuming various conditions for the gap parameters.

*Single d-wave order parameter: Its failure to describe the present results*. There is a general consensus that the superconducting order parameter symmetry in cuprates is not a simple $s$-wave type as is the case in conventional superconductors. A wealth of experimental results indicate unconventional pairing and more specifically point to the presence of nodes in the gap. A strong candidate which has been found to account for most of the properties in cuprates is a single complex $d$-wave order parameter with a gap of the form $\Delta(T)=\Delta_d(T)\cos2\phi$, where $\phi$ specifies the orientation of the two-dimensional momentum of the Cooper pairs. This expression leads to two important signatures, namely, the order parameter goes to zero in certain $k$ directions and also changes sign as one goes around the Fermi surface. Angle-resolved photoemission[27] and phase sensitive superconducting quantum interference device (SQUID) experiments[1] have shown strong evidence for this behavior. For experiments which measure quantities averaged over $k$ space (such as the microwave penetration depth), the consequence of the $d$-wave gap will lead to features in the low-temperature dependence which should be consistent with the presence of a finite density of states within the gap.

A linear low-temperature dependence in YBCO single crystals observed by the UBC group[21] [and subsequently confirmed by others including ourselves in YBCO (Refs. 18,28) and also Bi:2212 (Ref. 19)] has been claimed as prime evidence for nodes in the gap, which applies to

$d$-wave symmetry among other possibilities. Rigorous calculations of the microwave conductivity in the framework of $d$-wave theories have also been done to explain the features observed in prior YBCO/YSZ samples.[23,24]

In Fig. 3, a plot of $[\lambda^2(0)/\lambda^2(T)]$ vs reduced temperature $(t=T/T_c)$ for YBCO/YSZ single crystals is shown. A comparison to detailed $d$-wave calculations has been carried out by us in an earlier publication.[18] Comparison shows that although the low temperature dependence is reproduced by calculations (not shown) using a weak coupling $d$-wave order parameter, the agreement is not very good at temperatures $T>0.5T_c$, suggesting that strong coupling effects are needed.

For the YBCO/BZO single crystals, the low-temperature penetration depth $\lambda(T)$ is indeed linear for all three samples measured up to $\sim 20-25$ K with a characteristic slope $d\lambda/dT$ of about 4.5 Å/K similar to that of the YBCO/YSZ samples. However deviation from linearity is observed above 25 K for the YBCO/BZO crystals due to the onset of the broad 60 K bump. This is clearly evident from the plots of $\sigma_2(T)$ presented in Fig. 2 which shows a nonmonotonic dependence for AE103, AE180, and AE105 samples when compared to the AEXX curve. While a single order parameter may be reconciled at first glance for the YBCO/YSZ data,[18] it is impossible to do so for the results on the $BaZrO_3$ grown crystals.[7] Instead a two-component model has to be considered as is done below.

### B. Comparison to decoupled two-component order parameters

The simplest way in which one can analyze a two-component system is to consider two parallel superconducting channels and to add their complex conductivities. The total conductivity can then be written as

$$\sigma=\sigma_1-i\sigma_2=(\sigma_{1A}+\sigma_{1B})-i(\sigma_{2A}+\sigma_{2B}).$$

For ease of calculation we consider that the two components are decoupled with distinct transition temperatures $T_{cA}$ and $T_{cB}(>T_{cA})$. (The possibility of coupled components and $T_{cA}$ being a crossover temperature is discussed later). Calculations of the conductivities can be performed using the Mattis-Bardeen formalism introduced earlier. In an earlier paper, we had presented the qualitative model where for ease of calculation we used $s$-wave order parameters for both the $A$ and $B$ components.[7] In reality, it is essential to choose at least one component to be $d$ wave to produce the linear low temperature dependence. Using a combination of $s$ and $d$ gap symmetries, it is possible to obtain excellent quantitative fits to the observed experimental data for all the YBCO/BZO single crystals.

Figure 4 shows the experimental data for $\sigma_2$ and $\sigma_1$ along with the fits obtained with the two component model assuming an $s$ wave for the A component and $d$ wave for the B component. Good fits can also be obtained for $(d+d)$ and $(d+s)$ cases for the two (A+B) components. The data for the AE103 sample only is presented in the figures for clarity. It is possible to obtain similar fits for the other YBCO/BZO crystals and the fit parameters for all the samples are tabulated in Table II. A good agreement between the data and model is obvious. Best fits are obtained for the following *generic* choices.

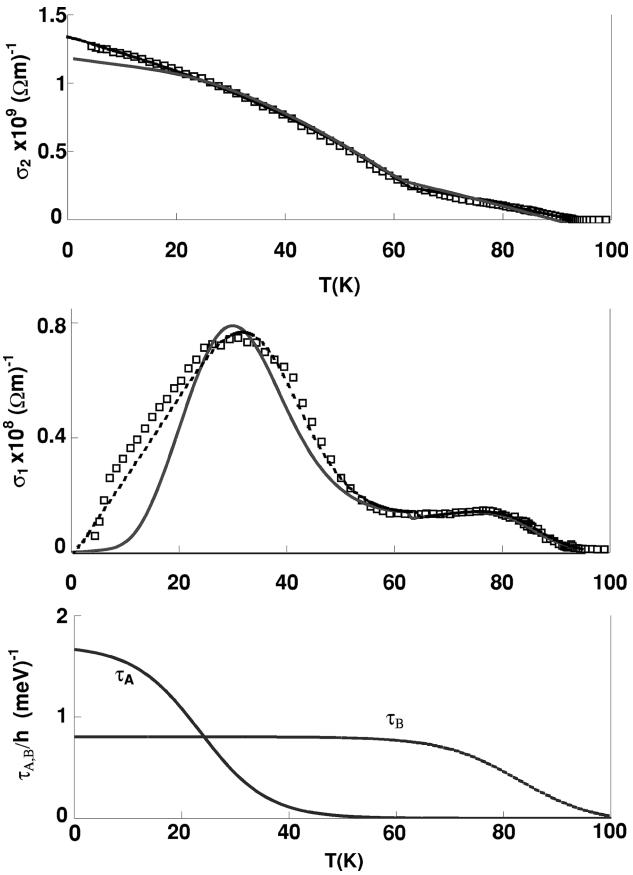


FIG. 4. $\sigma_2$ and $\sigma_1$ data for YBCO/BZO single crystal (AE103) along with the fits generated using a decoupled two-component model $(s+d)$ [solid line] and $(d+d)$ (dashed line), discussed in the text. The bottom panel shows the variation of scattering times $\tau_A$ and $\tau_B$ below the $T_c$ for A and B components for the $(s+d)$ case. Essentially similar fits can be obtained for $(d+s)$ case (not shown).

(1) A low temperature component $A$ with $T_{cA}\sim 60$ K and a high-temperature component $B$ with $T_{cB}\sim 93$ K.

(2) A weak coupling $d$-wave gap with $\Delta_B=2.16k_BT_c$ for the B component and an $s$-wave gap with $\Delta_A=1.76k_BT_c$ or a weak-coupling $d$-wave gap for the $A$ component.

(3) A lower fraction of $s$-wave ($\sim 0.3$) than the $d$-wave part ($\sim 0.7$).

(4) Temperature dependent scattering rates $\tau_{A,B}^{-1}\equiv\Gamma_{A,B}=\Gamma_{A,B(0)}(e^{\alpha(t-1)}-e^{-\alpha})+\Gamma^*_{A,B}$ were used for $\sigma_1$.[18,24] This exponential variation agrees with the suggestion that the scattering time increases rapidly below the transition temperature. The variation of $\tau_A$ and $\tau_B$ with temperature is plotted in bottom of Fig. 4. The detailed functional form is not as important as the key feature of rapid variation of $\tau_A$ below 65 K and $\tau_B$ below 93 K.

The two-component model also provides an explanation of the YBCO/YSZ data as can be seen from Fig. 5. The fit parameters (Table II) suggest that impurities suppress the order parameter for the A component [a smaller ratio 10% of the superfluid density $n_{sA}$ as well as a weaker gap $\Delta_A(0)/k_BT_{cA}\sim 1.0$ are needed], as well as greatly enhancing the scattering rate $\tau_B^{-1}$ about 10 times larger for the B component. The rapid variation of $\tau_A$ below 50 K is still needed to obtain the 30 K peak in $\sigma_1(T)$ for the YBCO/YSZ crystals.

TABLE II. Fit parameters for the three YBCO/BZO crystals using the several two-component scenarios. For the YBCO/YSZ case, fits shown in Fig. 5 using the two-component model are generated using the following parameters: Components: A(0.1) and B(0.9); $T_cA,B=60,92$ K; $\Gamma_{(A,B)(0)}=10,14$; $\alpha=7,12$; $\Gamma^*_{(A,B)}=0.1,0.01$. While the numbers are identical for $(s+d)$ and $(d+d)$ cases, $(d+s)$ does not fit the data.

| Samples | AE103 $(d+d)$ | AE105 $(d+d)$ | AE180 $(d+d)$ |
|---|---|---|---|
| Components | A(0.6), B(0.4) | A(0.6), B(0.4) | A(0.48), B(0.52) |
| $T_{c(A,B)}$ | 63, 93 K | 59, 93 K | 58, 93 K |
| $\Gamma_{(A,B)(0)}$ MeV | 11, 8 | 10, 13 | 7, 13 |
| $\alpha$ | 12, 25 | 10, 8 | 9, 14 |
| $\Gamma^*_{(A,B)}$ MeV | 0.08, 0.6 | 0.08, 1.1 | 0.06, 1.2 |
| Samples | AE103 $(s+d)$ | AE105 $(s+d)$ | AE180 $(s+d)$ |
| Components | A(0.6), B(0.4) | A(0.6), B(0.4) | A(0.45), B(0.55) |
| $T_{c(A,B)}$ | 63, 93 K | 59, 93 K | 58, 93 K |
| $\Gamma_{(A,B)(0)}$ MeV | 12, 8 | 18, 14 | 10, 16 |
| $\alpha$ | 11, 25 | 11, 6 | 10, 16 |
| $\Gamma^*_{(A,B)}$ MeV | 0.05, 0.8 | 0.04, 0.4 | 0.02, 1.4 |
| Samples | AE103 $(d+s)$ | AE105 $(d+s)$ | AE180 $(d+s)$ |
| Components | A(0.78), B(0.22) | A(0.78), B(0.22) | A(0.68), B(0.32) |
| $T_{c(A,B)}$ | 63, 93 K | 59, 93 K | 58, 93 K |
| $\Gamma_{(A,B)(0)}$ MeV | 20, 7 | 12, 9 | 10, 10 |
| $\alpha$ | 11, 21 | 11, 10 | 9, 14 |
| $\Gamma^*_{(A,B)}$ MeV | 0.24, 0.52 | 0.06, 0.01 | 0.1, 0.4 |

The occurrence of the low-temperature normal conductivity peak in $\sigma_1$ at around 30 K even though the superconducting transition temperatures are in excess of 90 K in YBCO crystals, has long been a puzzling feature. An exponential reduction of the quasiparticle scattering rate below $T_c$ was invoked to account for this. However, the present data provides an explanation for the location of this peak, since in the present experimental results, it is natural to associate the two $\sigma_1$ peaks with the corresponding features in the pair condensate density as inferred from $\sigma_2$. Two types of pairing with different characteristic energy scales are clearly observed in these high-quality YBCO/BZO single crystals. In the YBCO/YSZ samples, these energy scales are also present but their signatures are obscured by impurity scattering.

One aspect of the comparison should be noted. Because we have used a model in which the components are decoupled, the calculations necessarily show a sharp break at around $T_{cA}\sim 60$ K, whereas the data display a smooth crossover. This is an indication that the decoupled model is too simplistic, and a coupled model is necessary. Indeed such calculations performed[29] within a Ginzburg-Landau framework lead to a smooth crossover in $\lambda^{-2}(T)$ in closer agreement with the experiments. However, a full calculation of the conductivities requires a microscopic model which still needs to be implemented. (See also the remarks in the Summary section of this paper).

We note that there have been other discussions of multiple components (gaps or quasiparticles) in the cuprate superconductors. A two-gap model was proposed earlier by Klein *et al.*[30] to describe the data on YBCO thin films with low cation disorder. In their case, however, low and high gaps both with *s*-wave symmetry and the same $T_c$ were chosen to calculate the pair conductivity and the issue of $\sigma_1$ was not addressed in detail. Two-component behavior in 124 and underdoped 123 compounds have also been reported in Raman[31] and femtosecond optical response.[32]

Anisotropic penetration depth measurements along the *a* and *b* axes have been reported on untwinned YBCO/YSZ single crystals.[33] Lower $\lambda(0)$ in the *b* direction suggested superconductivity in the Cu-O chains with the onset $T_c$ same as that of the planes, viz. 93 K. The similarity between $1/\lambda_a^2$ and $1/\lambda_b^2$ was taken as evidence that chain order parameter also has nodes in the gap. However, in our present data, additional superfluid response clearly turns on *below* 60 K and if this is due to chains, then this would imply that chain superconductivity occurs at a lower temperature than the planes and would also directly contradict the conclusions reached in Ref. 33. Recent experiments on anisotropic thermal conductivity in detwinned YBCO/YSZ single crystals have also revealed enhanced superfluid density below $\sim$55 K which has been interpreted as due to chains.[34] This will be consistent with our observations of the microwave response in YBCO/BZO.

### C. Near-$T_c$ behavior

We turn our attention now to the transition region close to $T_c$. The temperature dependence of the penetration depth $\lambda(T)$ is expected to reveal the characteristic nature of the superconducting gap as it opens up and also possible contributions due to fluctuations. In contrast to conventional superconductors, the low dimensionality and small coherence length in cuprates make them good candidates for studying the effect of superconducting fluctuations and in determining the universality class they belong to. While Ginzburg-Landau theory generally describes the region near the transition very well in conventional superconductors, it has been argued that in YBCO assuming the simplest case of a *single*

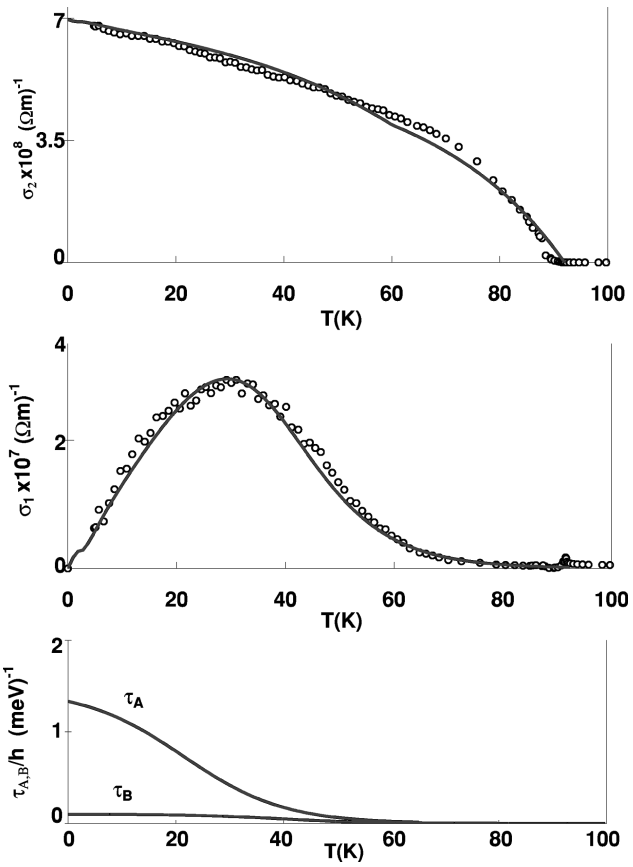


FIG. 5. $\sigma_2$ and $\sigma_1$ data for YBCO/YSZ single crystal (AEXX) along with the fits generated using a decoupled two-component model $(s+d)$ discussed in the text. The bottom panel shows the variation of scattering times $\tau_A$ and $\tau_B$ below the $T_c$ for A and B components for the $(s+d)$ case. The fit is identical with similar parameters for the $(d+d)$ case. The $(d+s)$ case does not fit the data.

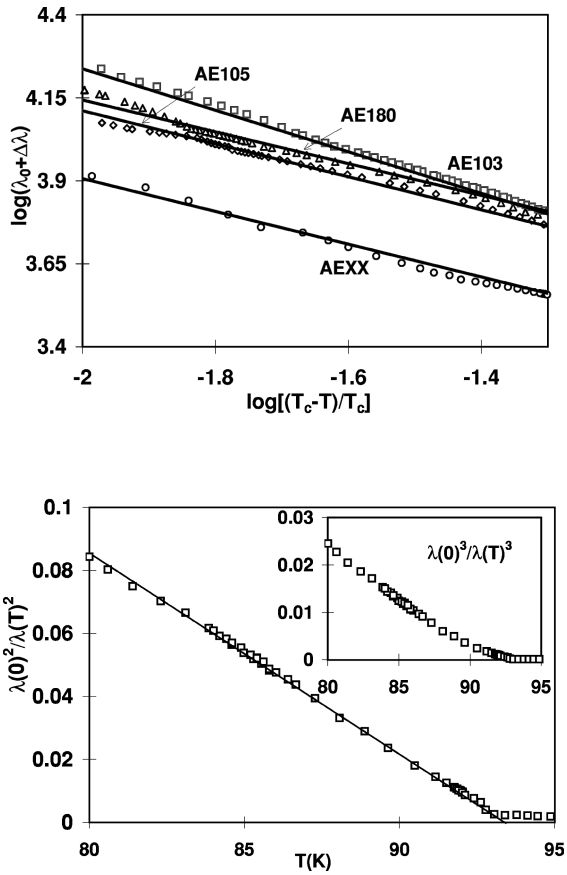


FIG. 6. Top panel: Penetration depth near $T_c$ shown in a log-log scale (logarithms are of base 10). The data sets indicate a similar variation in all four samples, with a slope of 0.5 indicating mean-field behavior. Bottom panel: Plot of the superfluid density $[\lambda(0)/\lambda(T)]^2$ vs $T$ just below $T_c$ for the AE103 crystal. The solid line is a guide to the eye indicating the linear variation consistent with mean-field behavior. Inset shows $[\lambda(0)/\lambda(T)]^3$ vs $T$ for the same data in which the curvature is clearly evident indicating disagreement with the 3D XY model.

complex order parameter, it is possible to observe critical behavior which would give rise to fluctuations corresponding to the universality class of the three-dimensional (3D) $XY$ model. Transport and thermodynamic measurements in the presence of a magnetic field have been interpreted in terms of this model.[35,36] However, this has also been disputed by Roulin *et al.*[37] who argue that fits of the specific heat near $T_c$ in YBCO single crystals for high magnetic fields do not rule out other explanations such as 3D lowest Landau level (LLL) scaling.

Penetration depth data close to the transition region will be influenced by the presence or absence of critical fluctuations. Specifically, a plot of $[\lambda(0)/\lambda(T)]^n$ as a function of $T$ just below $T_c$ is a useful indicator of the validity of standard mean-field or the 3D $XY$ models. While a mean-field behavior can be deduced if $[\lambda(0)/\lambda(T)]^2$ is linear in $T$, 3D $XY$ would require $[\lambda(0)/\lambda(T)]^3$ to be linear in $T$. The latter behavior has been observed in penetration depth measurements[38] and has been interpreted as consistent with the critical behavior of the 3D $XY$ model. It is important to note the choice of the range of temperature over which one looks for effects due to fluctuations is crucial. The dynamical fluctuations in the frequency dependent microwave conductivity near $T_c$ has been examined by Booth *et al.*[39] They arrive at the conclusion that while the Gaussian fluctuations can account for the behavior over a larger range in temperature, the region of critical fluctuations is restricted to a narrow range in temperature of 1–2 K below $T_c$ and an even smaller region above $T_c$.[40] It should be noted that the temperature dependence of $[\lambda(0)/\lambda(T)]^2$ from kinetic inductance measurements[41] and very recently from an inverted microstrip resonator technique[42] have shown mean-field dependence .

In a bid to investigate the transition region in our data on YBCO/BZO and YBCO/YSZ single crystals, we have plotted the penetration depth for all four crystals as a log-log plot against the reduced temperature $[(T_c-T)/T_c]$ shown in the top panel of Fig. 6. It is clear that all the data show a linear behavior (with a negative slope) with typical values of the slope lying around 0.5. The appropriate $\lambda(0)$ and $T_c$ values estimated from our $R_s$ and $X_s$ data for the three YBCO/BZO samples (AE103, AE180, AE105) and the YBCO/YSZ sample (AEXX) were taken to obtain the individual curves. Except the data for AE180 which has a slightly higher slope $(\sim 0.6)$, the other data form a set of parallel lines. This behavior is consistent with mean-field variation of the order parameter below $T_c$. To illustrate the point further, a plot of

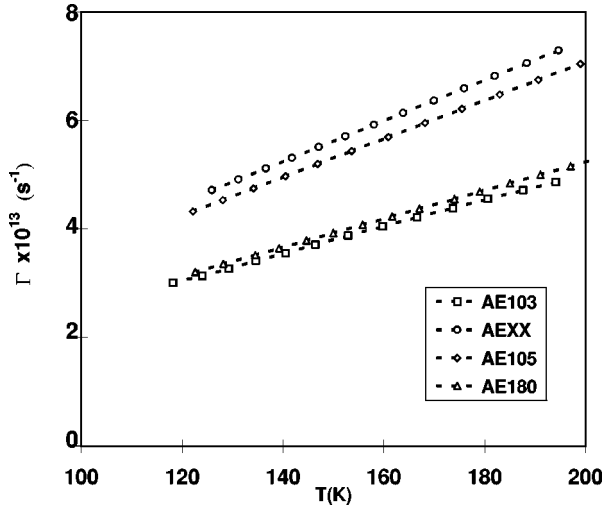


FIG. 7. The normal state inelastic scattering rate for all four samples. The data for AE103 and AE180 have lower values and smaller slope in comparison to AEXX and AE105 samples.

$[\lambda(0)/\lambda(T)]^2$ vs $T$ is presented in the bottom panel of Fig. 6 for one YBCO/BZO crystal. The *linear* variation is quite obvious and is clearly different from the behavior reported for YBCO single crystals in Ref. 37. The inset shows the same data plotted as $[\lambda(0)/\lambda(T)]^3$ vs $T$ which is nonlinear and rules out the possibility of 3D $XY$. The smooth variation of the $[\lambda(0)/\lambda(T)]^3$ vs $T$ curve also indicates against the possibility of interpretation as a crossover behavior from 3D $XY$ very near $T_c$ to a mean-field-like variation at lower temperatures. Our conclusion in this context would be that the near-$T_c$ behavior in all YBCO crystals is governed by a standard mean-field expression. In this respect, they seem to be similar to the conventional superconductors where the physical properties near $T_c$ are well described within the Ginzburg-Landau framework and the critical region is restricted to an unobservably small region near $T_c$. Alternatively, it is known that the presence of order parameter of mixed symmetry can give rise to fluctuations in the universality class other than 3DXY near $T_c$.[43] Our present results at low temperatures and the behavior near $T_c$ are consistent with this latter scenario.

### D. Normal state scattering rate

Assuming a local $j-\hat{E}$ relation in the skin depth limit, the normal state surface resistance can be written as $R_n=\sqrt{\omega\mu_0\rho_n/2}$ where the microwave normal state resistivity is expected to be the same as the dc resistivity and $\rho_n=2\Gamma\mu_0\lambda(0)^2$. Here $\lambda(0)$ is the London penetration depth and $\Gamma$ is the normal state scattering rate. Taking $\rho_n=\rho_0+\gamma T$ the resistivity values can be translated into the inelastic scattering rates given by $\Gamma=\gamma T/2\mu_0\lambda^2(0)$.

In Fig. 7, we have plotted the normal state inelastic scattering rate as a function of temperature for 100 K$<T<$200 K for all the YBCO/BZO samples along with the data for YBCO/YSZ crystal. Among the YBCO/BZO single crystals, the $\Gamma$ values as well as the slopes for AE103 and AE180 over the entire temperature range are lower than that for the AE105 sample. The YBCO/YSZ AEXX sample has the largest $\Gamma$ in this batch of crystals whose microwave surface impedance were measured in an identical manner. A comparison of this data with the $\sigma_1(T)$ data of Fig. 2 shows a clear correlation between the normal state scattering rate and the 80 K quasiparticle conductivity peak. This peak is prominent only in AE180 and AE103 samples which have a lower scattering rate, is suppressed in AE105 which shows a larger $\Gamma$ than the other two YBCO/BZO samples and practically absent in AEXX which has the largest scattering rate. This remarkable correlation indicates the sensitive nature of the conductivity peak to very small changes in impurity concentration and/or oxygen stoichiometry. Further studies in YBCO/BZO crystals with transition-metal doping and variation of oxygen stoichiometry are needed to explore the correlation between the electronic properties in the normal state and the quasiparticle contribution in the superconducting state which is suggested by our present data.

## IV. SUMMARY OF MICROWAVE PROPERTIES OF YBCO/BZO AND YBCO/YSZ CRYSTALS

We summarize below some of the microwave properties exhibited by the YBCO/BZO crystals along with comparison of results on the previous class of YBCO/YSZ samples. The key observations are as follows.

(1) The linear behavior of the low-temperature penetration depth $\lambda(T)\propto T$ appears to be very robust and is observed in all samples with essentially the same slope. $\lambda(T)$ rises linearly with $T$ upto $0.25T_c$ in YBCO/BZO single crystals with a characteristic slope $(d\lambda/dT)$ of about 4.5 Å/K. This linear variation which is widely observed[26,44,45] is in agreement with the observations on YBCO/YSZ crystals and more recently in magnetically aligned powders too and has been ascribed to the presence of nodes in the gap, and overall is considered a strong evidence for $d$-wave order parameter.[21] However, unlike the data in YBCO/YSZ, the full temperature dependence for YBCO/BZO display a characteristic bump feature around 60 K which points to the presence of an extra component in addition to a $d$-wave part.

(2) A linear behavior of $\lambda(T)$ is also seen in good quality BSCCO single crystals.[19,46,47] A $T^2$ behavior which has also been reported in YBCO thin films,[48] has been considered a consequence of inhomogeneties and additional scattering caused by impurities and disorder.

The surface resistance $R_s(T)$ of YBCO/BZO shows a bump at around 30 K as well as a broad bump at higher temperatures. In terms of conductivity, this results in two peaks occurring at ~30 and ~80 K. The ratio $\sigma_1/\sigma_n$ of the peaks are much higher (about 50 or more) and cannot be explained due to coherence effects predicted by BCS theory which yields a $\sigma_1/\sigma_n$ ratio typically around 2. We have associated these two peaks with two different quasiparticle systems corresponding to components A and B as discussed earlier.

In YBCO/YSZ, only the low-temperature peak at ~30 K is seen. This was first observed at sub-THz (Ref. 49) and at microwave frequencies.[50] To account for this feature, Bonn *et al.*[50] proposed a rapid increase in the inelastic scattering time $(\tau)$ below $T_c$ followed by a reduction in carrier density at low temperatures.

(3) A peak in $\sigma_1$ can arise due to an interplay of two effects, viz. a rapidly rising scattering time $\tau$ as temperature is lowered followed by a drop in the number of quasiparticles $n_{qp}$ as $T$ is lowered further.[49–51] A similar scenario is used in analyzing our present results on YBCO/BZO. Such an interpretation necessarily requires a rapid variation of $\tau_B$ just below 93 K and of $\tau_A$ below 65 K as is evident from Fig. 4 in YBCO/BZO.

It is to be noted that in BSCCO, our results[19] do not show any conductivity peak in $\sigma_1$ below $T_c$ but rather $\sigma_1/\sigma_n$ rises monotonically as $T$ is lowered. However, another study[46] claims to see a small reduction in $\sigma_1/\sigma_n$ at very low temperatures suggestive of a conductivity peak.

(4) It is important to note that *the two temperature scales of* 93 *and* 65 K are present in YBCO/YSZ *also*. This can be seen from the fact that two component analysis also describes the YBCO/YSZ data, as shown in Fig. 5, provided a suppressed $n_{sA}$ and $\tau_B$ are used. This suggests that in the YBCO/YSZ crystals, impurities lead to suppression of the pairing density of the A component, as well as greatly enhanced scattering of the B component.

(5) A very sharp peak in $\sigma_1$ just below $T_c$ at around 91–92 K is seen in all YBCO/BZO as well as YBCO/YSZ samples, so that there are a total of three conductivity peaks. This peak near $T_c$ has been ascribed to fluctuations[52] or inhomogeneities.[53] A quantitative analysis of this microwave conductivity peak in terms of fluctuations has been recently provided by Anlage *et al.*[40] In the YBCO/BZO samples this peak is extremely sharp and further attests to the high sample quality.

(6) The temperature scale of 65 K naturally raises the possibility of a multiphase sample with regions of $YBCO_{6.5}$. We have considered this issue very carefully and several experiments show that this is *conclusively* ruled out. *In situ* resistivity measurements at high temperatures have shown that the crystals can be reversibly oxygenated-deoxygenated, and that the diffusion constants are well characterized, indicating nothing unusual about the oxygenation of these samples.[8] Note also that the YBCO/YSZ sample AEXX was oxygenated using the same procedures but did not display the features in the conductivity. Furthermore, the similarity of the AE180 data with the other samples conclusively shows that even local O vacancies are not responsible for the present results. This is because in AE180, high-pressure oxygenation breaks up O deficient clusters, as evidenced by the elimination of the fishtail anomaly in samples prepared by this method.

(7) A comparison of the superfluid density for YBCO/YSZ and detwinned LuBCO/YSZ (shown in Fig. 3) indicates that twinning does not qualitatively affect the temperature dependence. However, the role of twinning in single crystals of YBCO/YSZ and YBCO/BZO in their microwave properties is an issue which needs to be explored further. Similar studies on detwinned YBCO/BZO crystals are the subject of future work.

(8) Our measurements on both YBCO/BZO and YBCO/YSZ single crystals are consistent with mean-field behavior rather than $3DXY$ close to $T_c$. Near-$T_c$ variation of $1/\lambda^2$ has been analyzed in terms of $3DXY$ scaling by Kamal *et al.*[38] in their YBCO/YSZ crystals. While a more rigorous study of the fluctuation contributions below and above $T_c$ by Booth *et al.*[39] indicated that $3DXY$ scaling is seen only over a limited temperature range, kinetic inductance measurements by Lemberger *et al.*[41] on thin films suggest mean-field behavior, in agreement with the conclusions of this paper.

(9) It should be noted that the pairing onset below 65 K in the $\sigma_2(T)$ is quite broad, and it is difficult to determine if it is the critical point of a phase transition. This interesting possibility of a second phase transition cannot be confirmed or ruled out by the present data and should be explored further in YBCO/BZO crystals. It should also be noted that it is likely that the order parameters are coupled and calculations of the superfluid density using a simple Ginzburg-Landau free energy for two coupled order parameters reproduce the main features of the $\lambda^{-2}(T)$ data.[29] At high temperatures $T_c > T > T_{cA}$, the symmetry is predominantly of type B, although a small A component is also induced due to the coupling. At lower temperatures $T < T_{cA}$, the A component grows so that both components (and hence a mixed symmetry) are present. It is likely that due to the subdominant nature of the A component, thermodynamic measurements such as specific heat do not reveal a large signature indicative of a sharp phase transition at 65 K. Some recent microscopic calculations indicate that the thermodynamic signatures, such as specific heat cusps, are weaker in the subdominant channels which appear at lower temperatures than in the main channel.[54]

(10) While we have presented a simple phenomenological two-component model in this paper to account for the two conductivity peaks in YBCO/BZO, microscopic calculations (similar to those based on a single $d$-wave order parameter[22–24]) need to be done for the surface impedance of a two-component superconductor. Very recently, a two-band model has been proposed to account for our observations in YBCO/BZO.[55] Varying a single parameter, viz., the interband scattering, it is possible to qualitatively reproduce the features seen in $\sigma_1$ and $\sigma_2$ of both YBCO/BZO and YBCO/YSZ. Furthermore, the analysis used here assumes phase coherence throughout the sample and does not include contributions arising from phase fluctuations.[56,57]

## V. RELATION TO MICROSCOPIC THEORIES

Models based on any type of mixed order parameter symmetry would yield results consistent with our experimental observations in the YBCO/BZO system. Mixed order parameter symmetry and multicomponent behavior of the order parameter has been addressed in several theoretical papers which can be broadly classified along the following categories.

(1) $s+d$, $s+id$. It has been argued that the orthorhombic structure of YBCO naturally leads to a mixing of $s$ and $d$ order parameter components.[3] Several theories[54,58–61] advocate to this general concept of a mixed $s+d$ order parameter and have successfully developed models which can describe the experimental results in YBCO. This appears to be consistent with photoemission data on overdoped BSCCO also.[62,58] Phenomenological[44] and microscopic theories[50] have been considered. The work of Ref. 63 indicates that the system likely goes from a $d$-wave state at high temperatures to an $s+id$ state at low $T$.

(2) *Chain-plane coupling.* The presence of Cu-O chains in

addition to planes raises the possibility of different superconducting condensates with different pairing energies residing on chains and planes. This can effectively lead to a two-component system exhibiting two different gaps.[64] Coupling between chain and plane bands has been proposed[65] to account for both the *s* and *d* characteristics displayed by YBCO.

(3)*Multiband models and Fermi pockets*. Theoretical treatments based on multiband models have been presented which considers the interband interactions.[65–69] This general framework also reproduces the essential features of a two-component superconductor. The nature of the Fermi surface could be important in determining the possibility of multiple pairing energies. The presence of pockets with *d*- and *g*-wave symmetries has been recently discussed.[70]

(4) *Surface states and time reversal symmetry breaking.* The possibility of mixed order parameter symmetry at the surface leading to breaking time reversal symmetry has been suggested.[71,72] Recent observation of Andreev bound states at the surface of YBCO (Refs. 73 and 74) strongly suggests this possibility.

(5) *Interlayer tunneling.* In a recent paper, Xiang and Wheatley[75] presented a model based on proximity effect incorporating a microscopic pair tunneling process which couples the Cu-O chains and planes in YBCO, to account for the experimental results on YBCO/YSZ data from the UBC group.[33] Our present results on the YBCO/BZO crystals suggests that within the interlayer tunneling model, single electron tunneling processes could account for the features observed in our data.

## VI. CONCLUSION

In summary, we have shown that high-quality single crystals of YBCO grown in $BaZrO_3$ crucibles exhibit features in their microwave properties, which are inconsistent with a pure *d*-wave order parameter and instead point to the occurrence of multicomponent superconductivity. The measurements reveal the presence of two pairing temperatures corresponding to two superconducting (pair/quasiparticle) components in the optimally doped compound. This should be borne in mind and careful studies should be performed on high-quality materials to further explore these issues.

## ACKNOWLEDGMENTS

Work at Northeastern was supported by NSF-DMR-9623720, and at Geneva by the Fonds National Suisse de la Recherche Scientifique. We thank Alain Junod, R. S. Markiewicz, Balam A. Willemsen, and D. P. Choudhury for useful discussions.

[1] See D. J. Harlingen, Rev. Mod. Phys. **67**, 515 (1995), and references therein.
[2] K. A. Muller, Nature (London) **377**, 133 (1995).
[3] B. E. C. Koltenbah and R. Joynt, Rep. Prog. Phys. **60**, 23 (1997).
[4] A. Erb, E. Walker, and R. Flükiger, Physica C **245**, 245 (1995).
[5] H. Casalta, P. Schleger, P. Harris, B. Lebech, N. H. Andersen, R. Liang, P. Dosanjh, and W. N. Hardy, Physica C **258**, 321 (1996).
[6] H. Ikuta and D. M. Ginsberg, J. Supercond. **9**, 259 (1996).
[7] H. Srikanth, B. A. Willemsen, T. Jacobs, S. Sridhar, A. Erb, E. Walker, and R. Flükiger, Phys. Rev. B **55**, R14 733 (1997).
[8] A. Erb, B. Greb, and G. Müller-Vogt, Physica C **259**, 83 (1996).
[9] B. G. Storey, M. A. Kirk, and L. D. Marks, Physica C **246**, 46 (1995).
[10] E. Brecht, W. W. Schmahl, M. Rodewald, G. Miehe, H Fuess, N. H. Andersen, J. Hanssmann, and Th. Wolf, Physica C **265**, 53 (1996).
[11] I. Maggio-Aprile, Ch. Renner, A. Erb, E. Walker, and Ø. Fischer, Phys. Rev. Lett. **75**, 2754 (1995).
[12] A. Erb, J.-Y. Genoud, F. Marti, M. Däumling, E. Walker, and R. Flükiger, J. Low Temp. Phys. **105**, 1023 (1996).
[13] J.-Y. Genoud,M. Roulin, B. Revaz, A. Erb, A. Mirmelstein, G. Triscone, and A. Junod, Czech. J. Phys. **47**, 1047 (1997).
[14] I. Maggio-Aprile, Ch. Renner, A. Erb, E. Walker, and O. Fischer, J. Low Temp. Phys. **105**, 1129 (1996).
[15] A. Junod, J.-Y. Genoud, B. Revaz, A. Erb, and E. Walker, Physica C **275**, 245 (1997); M. Roulin, A. Junod, A. Erb, and E. Walker, J. Low Temp. Phys. **105**, 1099 (1996).
[16] M. V. Indenbom, C. J. van der Beek, V. Berseth, W. Benoit, G. D'Anna, A. Erb, E. Walker, and R. Flükiger, Nature (London) **385**, 702 (1997).
[17] S. Sridhar and W. L. Kennedy, Rev. Sci. Instrum. **59**, 531 (1988).
[18] T. Jacobs, S. Sridhar, C. T. Rieck, K. Scharnberg, T. Wolf, and J. Halbritter, J. Phys. Chem. Solids **56**, 1945 (1995).
[19] T. Jacobs, S. Sridhar, Qiang Li, G. D. Gu, and N. Koshizuka, Phys. Rev. Lett. **75**, 4516 (1995).
[20] J. Buan, C. C. Huang, A. M. Goldman, Oriol T. Valls, T. Jacobs, N. Israeloff, S. Sridhar, C. R. Shih, Branko P. Stojkovic, J.-Z. Liu, Robert Shelton, and H. D. Yang, Phys. Rev. B **45**, 7462 (1996).
[21] W. N. Hardy, D. A. Bonn, D. C. Morgan, R. Liang, and K. Zhang, Phys. Rev. Lett. **70**, 3999 (1993).
[22] R. A. Klemm, K. Scharnberg, D. Walker, and C. T. Rieck, Z. Phys. B **72**, 139 (1988).
[23] P. J. Hirschfeld, W. O. Puttika, and D. J. Scalapino, Phys. Rev. B **50**, 10 250 (1994).
[24] S. Hensen, G. Müller, C. T. Rieck, and K. Scharnberg, Phys. Rev. B **56**, 6237 (1997).
[25] J. R. Waldram, *Superconductivity of Metals and Cuprates* (IOP, Bristol, 1996).
[26] D. C. Mattis and J. Bardeen, Phys. Rev. **111**, 412 (1958).
[27] Z.-X. Shen, D. S. Dessau, B. O. Wells, D. M. King, W. E. Spicer, A. J. Arko, D. Marshall, L. W. Lombardo, A. Kapitulnik, P. Dickinson, S. Doniach, J. diCarlo, A. G. Loeser, and C. H. Park, Phys. Rev. Lett. **70**, 1553 (1993).
[28] J. Mao, D. H. Wu, J. L. Peng, R. L. Greene, and S. M. Anlage, Phys. Rev. B **51**, 3316 (1995).
[29] S. Sridhar (unpublished).
[30] N. Klein, N. Tellman, H. Schulz, K. Urban, S. A. Wolf, and V. Z. Kresin, Phys. Rev. Lett. **71**, 3355 (1993).
[31] E. T. Heyen, M. Cardona, J. Karpinski, E. Kaldis, and S. Rusiecki, Phys. Rev. B **43**, 12 958 (1991).

[32] C. J. Stevens, D. Smith, C. Chen, J. F. Ryan, B. Pobodnik, D. Mihailovic, G. A. Wagner, and J. E. Evetts, Phys. Rev. Lett. **78**, 2212 (1997).
[33] K. Zhang, D. A. Bonn, R. Liang, and W. N. Hardy, Phys. Rev. Lett. **73**, 2484 (1994).
[34] R. Gagnon, S. Pu, B. Ellman, and L. Taillefer, Phys. Rev. Lett. **78**, 1976 (1997).
[35] M. B. Salamon, J. Shi, N Overend, and M. A. Howson, Phys. Rev. B **47**, 5520 (1993).
[36] N. Overend, M. A. Howson, and I. D. Lawrie, Phys. Rev. Lett. **72**, 3238 (1994).
[37] M. Roulin, A. Junod, and J. Muller, Phys. Rev. Lett. **75**, 1869 (1995).
[38] S. Kamal, D. A. Bonn, N. Goldenfeld, P. J. Hirschfeld, R. Liang, and W. N. Hardy, Phys. Rev. Lett. **73**, 1845 (1994).
[39] J. C. Booth, D. H. Wu, S. B. Qadri, E. F. Skelton, M. S. Osofsky, A. Piqué, and S. M. Anlage, Phys. Rev. Lett. **77**, 4438 (1996).
[40] S. M. Anlage, J. Mao, J. C. Booth, D. H. Wu, and J. L. Peng, Phys. Rev. B **53**, 2792 (1996).
[41] T. R. Lemberger, E. R. Ulm, K. M. Paget, and V. C. Matijasevic, Proc. SPIE **2696**, 211 (1996).
[42] A. Andreone, C. Cantoni, A. Cassinese, A. Di Chiara, and R. Vaglio, Phys. Rev. B **56**, 7874 (1997).
[43] J. F. Annett, N. D. Goldenfeld, and S. R. Renn, in *Physical Properties of High Temperature Superconductors II*, edited by D. M. Ginsberg (World Scientific, New Jersey, 1990).
[44] C. Panagopoulos, J. R. Cooper, N. Athanassopoulou, and J. Chrosch, Phys. Rev. B **54**, R12 721 (1996).
[45] C. W. Chu, Y. Y. Xue, Y. Cao, and Q. Xiong, J. Phys. Chem. Solids **56**, 1887 (1995).
[46] S-F. Lee, D. C. Morgan, R. J. Ormeno, D. M. Broun, R. A. Doyle, and J. R. Waldram, Phys. Rev. Lett. **77**, 735 (1996).
[47] T. Shibauchi, N. Katase, T. Tamegai, and K. Uchinokura, Physica C **254**, 227 (1996).
[48] Z. Ma, R. C. Taber, L. W. Lombardo, A. Kapitulnik, M. R. Beasley, P. Merchant, C. B. Eom, S. Y. Hou, and J. M. Phillips, Phys. Rev. Lett. **71**, 781 (1993).
[49] M. C. Nuss, P. M. Mankiewich, M. L. O'Malley, E. H. Westerwick, and P. B. Littlewood, Phys. Rev. Lett. **66**, 3305 (1991).
[50] D. A. Bonn, P. Donsajh, R. Liang, and W. N. Hardy, Phys. Rev. Lett. **68**, 2390 (1992).
[51] T. Jacobs, K. Numssen, R. Schwab, R. Heidinger, and J. Halbritter, IEEE Trans. Appl. Supercond. **7**, 1917 (1997).
[52] M. L. Horbach, W. van Sarloos, and D. A. Huse, Phys. Rev. Lett. **67**, 3464 (1991).
[53] H. K. Olsson and R. H. Koch, Phys. Rev. Lett. **68**, 2406 (1992).
[54] E. Otnes and A. Sudbo (unpublished).
[55] A. A. Golubov and M. R. Trunin (private communication).
[56] V. J. Emery and S. A. Kivelson, Nature (London) **374**, 434 (1995).
[57] E. Roddick and D. Stroud, Phys. Rev. Lett. **74**, 1430 (1995).
[58] J. Betouras and R. Joynt, Europhys. Lett. **1**, 119 (1995)
[59] C. O'Donovan and J. P. Carbotte, Phys. Rev. B **52**, 16 208 (1995).
[60] M. T. Beal-Monod and K. Maki, Phys. Rev. B **53**, 5775 (1996).
[61] D. van der Marel, Phys. Rev. B **51**, 1147 (1995).
[62] J. Ma, C. Quitmann, R. J. Kelley, H. Berger, G. Margaritondo, and M. Onellion, Science **267**, 862 (1995).
[63] Y. Ren, W. Xu, and C. S. Ting, Phys. Rev. B **53**, 2249 (1996).
[64] V. Z. Kresin and S. A. Wolf, Phys. Rev. B **46**, 6458 (1992).
[65] R. Combescot and X. Leyronas, Phys. Rev. Lett. **75**, 3732 (1995).
[66] P. H. Dickinson and S. Doniach, Phys. Rev. B **47**, 11 447 (1993).
[67] R. Combescot, cond-mat/9707241 (unpublished).
[68] A. A. Golubov, M. R. Trunin, A. A. Zhukov, O. V. Dolgov, and S. V. Shulga, J. Phys. I **6**, 2275 (1996).
[69] P. K. Mohanty and A. Taraphder, cond-mat/9703180 (unpublished).
[70] P. V. Shevchenko and O. P. Sushkov, cond-mat/9705129 (unpublished).
[71] R. B. Laughlin, Physica C **234**, 280 (1994).
[72] A. M. Tikofsky and D. B. Bailey, Phys. Rev. B **52**, 9194 (1995).
[73] M. Covington, M. Aprili, E. Paraoanu, L. H. Greene, F. Xu, J. Zhu, and C. A. Mirkin, Phys. Rev. Lett. **79**, 277 (1997).
[74] M. Fogelstrom and D. Rainer, Phys. Rev. Lett. **79**, 281 (1997).
[75] T. Xiang and J. M. Wheatley, Phys. Rev. Lett. **76**, 134 (1996).